05

Spatial organization of sodium nitrite nanoparticles in porous glass with interface modified by titanium dioxide

© O.A. Alekseeva[1], M.V. Tomkovich[1], A.A. Naberezhnov[1], A.A. Sysoeva[1], Yu.E. Gorshkova[2,3]

[1] Ioffe Institute, St. Petersburg, Russia
[2] Frank Neutron Physics Laboratory, Joint Nuclear Research Institute, Dubna, Moscow oblast, Russia
[3] Kazan Federal University, Kazan, Russia
E-mail: alekseeva.oa@mail.ioffe.ru

Received October 16, 2024
Revised November 28, 2024
Accepted November 29, 2024

The results of a study of the effect of titanium oxide modification of the porous glass sodium nitrite interface on the spatial organization of $NaNO_2$ nanoparticles obtained by introducing sodium nitrite from an aqueous solution into the pore space of a mesoporous glass matrix with an average channel (pore) diameter of 6(1) nm (PG6) are presented. It is shown, that in the nanocomposite (NCM) PG6+$NaNO_2$ sodium nitrite forms nanoagglomerates with a radius of gyration of 68 nm, in which the amorphous and crystalline phases coexist. On a spatial scale from 2 to 27 nm, a surface fractal-type structure is realized in this NCM, described by the scattering law $I(Q) \sim Q^{-\alpha}$ (Q is the transferred momentum) with $\alpha = 3.57(2)$. The sizes of coherent scattering regions for sodium nitrite nanoparticles in PG6+$NaNO_2$ and PG6+TiO_2+$NaNO_2$ nanocomposites (~ 10 nm) have been determined.

Keywords: sodium nitrite, nanocomposite materials, crystal structure, small-angle X-ray scattering, X-ray diffraction, interface.

DOI: 10.61011/TPL.2025.04.60993.20154

Several factors leading to significant changes in the properties of nanostructured materials (compared to the properties of their bulk counterparts) are known. One of these is the influence of the interface that modifies the properties of nanocomposite materials (NCMs). In the present study, alkali-borosilicate glasses (ABSs) were used as a matrix for the production of NCMs; the procedure for fabrication of such mesoporous matrices was detailed in [1,2]. Following partial acid etching of through interconnected channels (their average diameter in our ABSs was $\langle D \rangle \sim 45(5)$ nm) filled with a chemically unstable phase, a mesoporous matrix with a dendritic 3D network of pores (voids) was formed. The average pore diameter in the obtained PG6 matrix was determined to be $\langle d \rangle \sim 6(1)$ nm based on mercury porosimetry data. The total volume (porosity of the sample) of these voids was $\sim 25\%$ of the sample volume. $NaNO_2$ was used as the „guest" substance. Its properties and structural evolution have been studied extensively for both the bulk material and NCMs [3–8]. The fabrication of a titanium dioxide interface was detailed in [9]. The average pore diameter decreases to ~ 4 nm in the process, but their through dendritic structure is preserved. TiO_2 itself forms one or two amorphous material layers on the surface of PG6 pores. $NaNO_2$ was introduced into the voids of PG6 and PG6+TiO_2 matrices from a saturated aqueous solution [9]; in both samples, 59% of the initial PG6 pore volume were filled with $NaNO_2$. It was demonstrated in [9] that the presence of titanium dioxide in pores has a profound effect on the dielectric properties of PG6+TiO_2+$NaNO_2$ nanocomposites, which change radically compared to those of PG6+$NaNO_2$. This effect may be associated with a change in spatial organization and phase composition of the PG6+TiO_2+$NaNO_2$ NCM. Therefore, the aim of the present study was to perform a step-by-step examination of the evolution of spatial NCM organization along the following chain: empty PG6 glass→PG6+TiO_2→PG6+TiO_2+$NaNO_2$. The crystal structure of PG6+$NaNO_2$ and PG6+TiO_2+$NaNO_2$ samples was studied using a SuperNova Oxford Diffraction ($\lambda = 0.71$ Å, Mo$K_{\alpha 1}$) X-ray diffractometer. Measurements were carried out in transmission (the plate thickness was 0.5 mm); the exposed region of the samples was $\sim 200\,\mu m^2$ in size. The background from the amorphous framework of empty PG6 and for the PG6+TiO_2 NCM was measured separately. The spatial characteristics of the PG6+TiO_2+$NaNO_2$ sample were studied by small-angle X-ray scattering (SAXS) at the Xeuss 3.0 setup (JINR, LNP, Dubna, $\lambda = 0.71$ Å) at three different sample−detector distances: 550, 1825, and 4605 mm. Figure 1 presents the diffraction patterns for the PG6+$NaNO_2$ and PG6+TiO_2+$NaNO_2$ NCM samples (the corresponding backgrounds from empty PG6 and PG6+TiO_2 were subtracted). The structure corresponds to $NaNO_2$, but Bragg peaks are broadened strongly due to the size effect. Having analyzed the peak widths, we determined sizes $\langle L_{1,2} \rangle$ of the coherent scattering regions (CSRs), which characterize the size of $NaNO_2$ nanoparticles in NCMs: $\langle L_1 \rangle = 9(1)$ nm for PG6+$NaNO_2$ and $\langle L_2 \rangle = 12(3)$ nm for PG6+TiO_2+$NaNO_2$ (inset in Fig. 1). Figure 1 shows clearly that the integral intensity of Bragg peaks increases sharply for the PG6+TiO_2+$NaNO_2$ NCM: it is approximately 4.5 times higher than the one for PG6+$NaNO_2$. Since the degree of filling of the pore

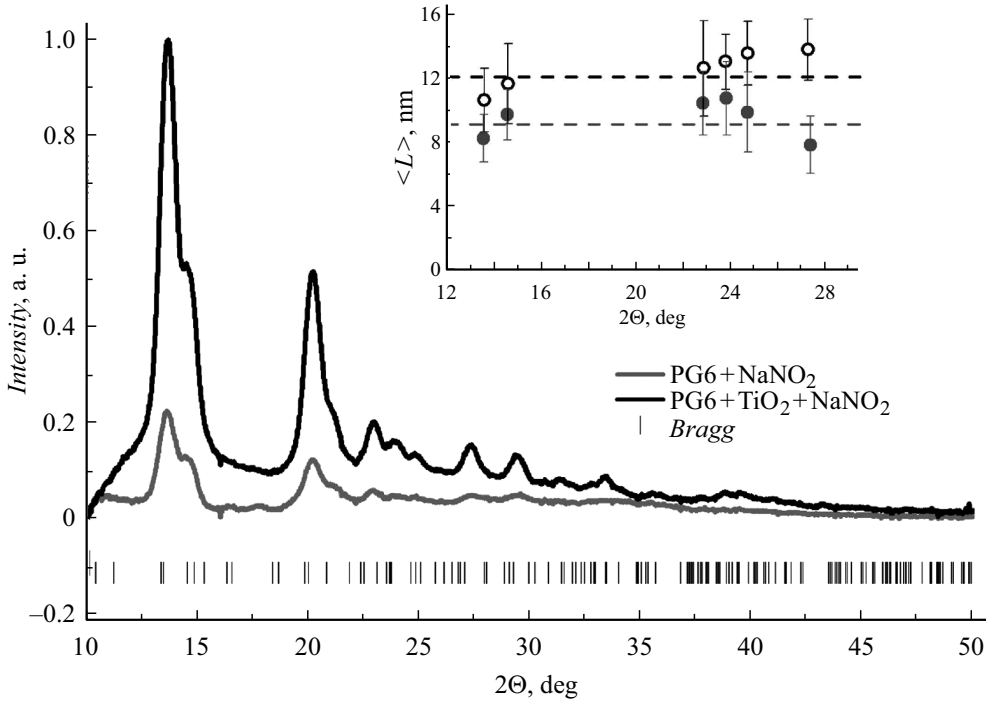

Figure 1. Room-temperature diffraction patterns for PG6+$NaNO_2$ (gray curve) and PG6+TiO_2+$NaNO_2$ (black curve) NCMs. The dashes at the bottom indicate the positions of peaks. The inset shows sizes $\langle L \rangle$ of the coherent scattering region for $NaNO_2$ in PG6+$NaNO_2$ (dark symbols) and PG6+TiO_2+$NaNO_2$ (light symbols) NCMs.

space, the geometric dimensions of the samples, and the measurement geometry were the same for both NCMs, the intensity was logically expected to increase by a factor of $(L_2/L_1)^3 \approx 2.35$ (instead of 4.5) due to an increase in the CSR size. This fact supports the assumption that the presence of titanium dioxide contributes to an increase in the fraction of crystalline sodium nitrate in the PG6+TiO_2+$NaNO_2$ NCM. This also implies that both samples contain an amorphous phase of sodium nitrite, as was suggested in [9]. SAXS studies of the spatial organization of the PG6+TiO_2+$NaNO_2$ NCM were performed next. The spatial characteristics of PG6 and PG6+TiO_2 matrices were determined in [10]. It is known [11] that the SAXS intensity at large transferred momenta $Q = \frac{4\pi}{\lambda}\sin\theta$ ($QR_g \geqslant 1$ is the Porod's region, where R_g is the radius of gyration, the root-mean-square radius of inertia of a scattering particle) is written as

$$I(Q) = AQ^{-\alpha} + B, \qquad (1)$$

where A and B are constants and B is the background at large Q. Constant A contains a difference in scattering amplitude density (contrast) $(\Delta\rho)^2 = (\rho_p - \rho_s)^2$, where ρ_p and ρ_s are the scattering densities for the material in pores and the matrix material [12]. In the case of highly branched surfaces (surface fractals), $3 < \alpha < 4$ [12]. The value of $\alpha = 4$ corresponds to scattering by a smooth surface (Porod's law). At $QR_g < 1$ (Guinier region), the following relation holds true:

$$I(Q) = I(0)\exp\left(-(Q^2R_g^2)/3\right). \qquad (2)$$

The value of $1 < \alpha < 3$ corresponds to the presence of a mass fractal with dimension $D_v = \alpha$, while $4 < \alpha < 6$ implies scattering by a diffuse surface [13]. Expression $d = 2\pi/Q$ is sufficient for a transition to direct space. Figure 2 presents the dependences of intensity $I(Q)$ for empty glass PG6 and the PG6+TiO_2+$NaNO_2$ NCM. The $I(Q)$ dependence for the NCM differs sharply from that for empty PG6 and PG6+TiO_2 [10]. In the region spanning from $Q_1 = 0.023\,\text{Å}^{-1}$ ($d = 273\,\text{Å}$) to $Q_2 = 0.26\,\text{Å}^{-1}$ ($d = 24\,\text{Å}$), $I(Q)$ follows closely the $Q^{-\alpha}$ law with $\alpha = 3.57(2)$; i.e.,a spatial structure similar to a surface fractal is established on this scale in direct space in PG6+TiO_2+$NaNO_2$. Using expression (2), we determined $R_g = 68(2)$ nm for $NaNO_2$ nanoagglomerates in PG6+TiO_2+$NaNO_2$. The presence of a correlation peak in $I(Q)$ for unfilled PG6 with a maximum at $Q_{\max} \sim 0.02\,\text{Å}^{-1}$ is typical for porous glasses [14,15] and is attributable to the process of spinodal decomposition [16] of the two-phase system of the initial borosilicate glass [1,2], which leads to the formation of structural units in the matrix with characteristic size $D \sim 2\pi/Q_{\max}$, where $Q_{\max}$ is the position of the maximum of this peak. The correlation peak in the PG6+TiO_2+$NaNO_2$ NCM shifts strongly toward smaller Q, which is associated with the emergence of additional interfaces. The peak itself is characterized well by squared Lorentzian

$$I(Q) = A_1/\left((Q_{\max 0} - Q)^2 + \kappa^2\right)^2 + B_1, \qquad (3)$$

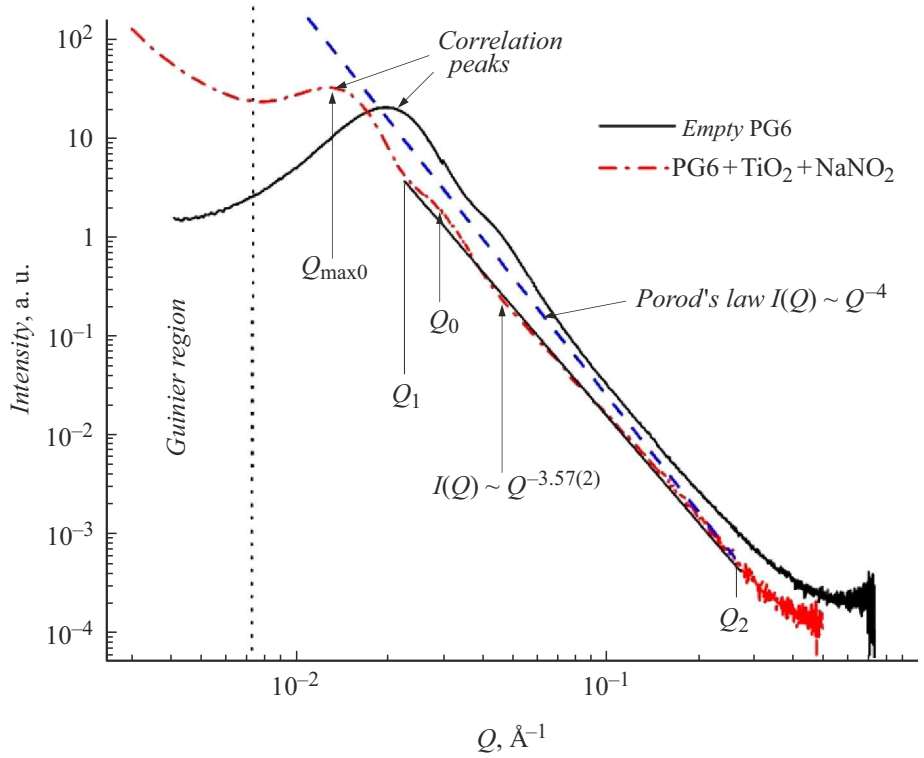

Figure 2. Dependences $I(Q)$ for empty PG6 (solid curve) and the PG6+TiO_2+$NaNO_2$ NCM (dash-and-dot curve). The dashed line represents Porod's law $I(Q) \sim Q^{-4}$. The straight line between Q_1 and Q_2 marks the region where law $I(Q) \sim Q^{-3.57}$ holds for scattering by the PG6+TiO_2+$NaNO_2$ NCM.

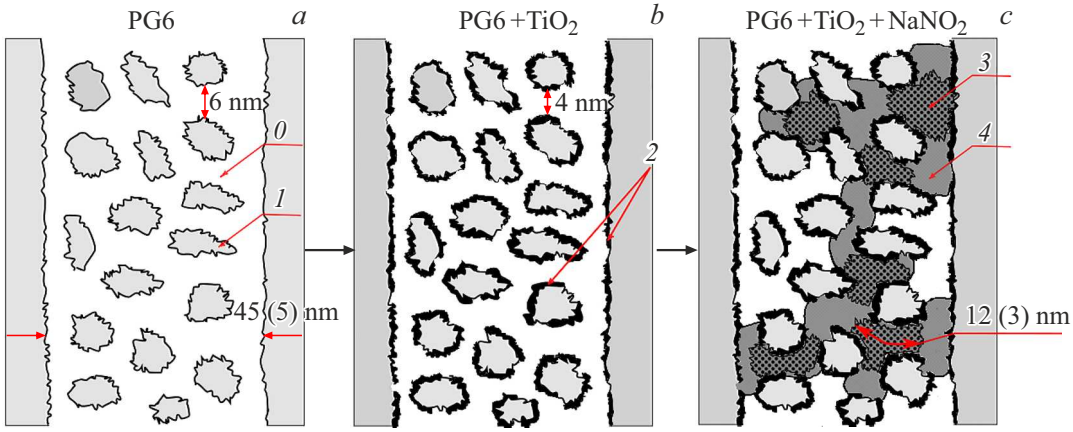

Figure 3. Diagram of spatial organization of sodium nitrite nanoagglomerates in the PG6+TiO_2+$NaNO_2$ NCM (*a*–*c*). Gray regions on the left and right in all panels correspond to the PG6 matrix framework. Size $L_2 = 12(3)$ nm of the coherent scattering region is indicated in panel *c*.

where A_1 is a constant, B_1 is the background, $Q_{\max 0} = 0.01264(2)\,\text{Å}^{-1}$ is the position of the maximum, and $\kappa = 0.0078(2)\,\text{Å}^{-1}$ is the inverse correlation radius (correlation radius $r_c = 2\pi/\kappa$). In direct space, the squared Lorentzian corresponds to a correlation function of the form $F(r) = \exp(-\kappa r)$. The presence of this peak indicates that $NaNO_2$ features local ordering with $r_c \approx 80$ nm on scale $L = 2\pi/Q_{\max 0} \approx 50$ nm. The „shoulder" in dependence $I(Q)$ for the NCM at Q_0 is associated with the residual contribution of the correlation peak from PG6. Thus, the establishment of spatial organization of $NaNO_2$ agglomerates in this NCM may be presented schematically as a sequence shown in Figs. 3, *a*–*c*.

1. Following the first stage of acid etching [1], a multiconnected 3D structure of secondary silica and etching reaction products is established in channels of the matrix framework with $\langle D \rangle \sim 45$ nm. This structure is presented in the illustrated section in the form of „islands" (*1* in

Fig. 3, *a*). The empty space (*0* in Fig. 3, *a*) between the „islands" of secondary silica and the walls of a channel with $\langle D \rangle = 45$ nm forms a 3D network of cavities (pores) with an average diameter of 6 nm.

2. When an interface is created, a TiO_2 layer (*2* in Fig. 3, *b*) forms on the surfaces of channels and secondary silica, and the average diameter of channels decreases (~ 4 nm) [9]. According to the SAXS data [10], α for PG6+TiO_2 decreases sharply (to 3.21(2)) in the Porod's region relative to the corresponding α value for PG6 (close to 4) [10]. In the case of nanoparticles of TiO_2 $R_{g1} = 15(2)$ nm [10]; i.e., titanium dioxide in the pores of PG6 glass forms a surface fractal in several adjacent pores with an average diameter of ~ 4 nm that consists of interconnected hollow cylinders. The empty space inside them is filled with $NaNO_2$ at the next stage.

3. In PG6+TiO_2+$NaNO_2$ α increases from 3.21(2) to 3.57(2) in the Porod's region (the surface fractal becomes „smoother"), while $R_g \sim 68$ nm exceeds significantly the CSR size for $NaNO_2$ particles determined from diffraction data. Since $I(Q)$ is governed by contrast $(\Delta\rho)^2$ rather than by the aggregate state of the scatterer, crystalline and amorphous phases of $NaNO_2$ have the same contrast. In this case, the most likely scenario is as follows: as the pore space is filled, large agglomerates of sodium nitrite, which consist of smaller nanoparticles of the crystalline phase (*3* in Fig. 3, *c*) located inside more extended 3D regions of the amorphous phase (*4* in Fig. 3, *c*), form there. It bears reminding that the presence of titanium dioxide increases the fraction of crystalline $NaNO_2$ in pores compared to the case of the PG6+$NaNO_2$ NCM. If we assume that the region of local ordering with $r_c \approx 80$ nm and a dendritic 3D structure established in several neighboring interconnected channels with $\langle D \rangle \sim 45$ nm may be inscribed in a sphere with a certain characteristic R_{g0}, then R_{g0} may be estimated using the formula for the radius of gyration for a sphere. Let us take r_c as the effective size of the region. Relation $(R_{g0})^2 = 3/5(r_c)^2$ [17] then yields $R_{g0} \approx 62$ nm. This agrees closely with the $R_g = 68(2)$ nm value obtained from the analysis of SAXS data in the Guinier region. The proposed model of spatial organization of sodium nitrite in the PG6+TiO_2+$NaNO_2$ sample explains well the features of dielectric response of this NCM observed in [9].

Funding

This study was supported financially by the Russian Science Foundation (grant № 23-22-00260, https://rscf.ru/project/23-22-00260/).

Conflict of interest

The authors declare that they have no conflict of interest.

References

[1] O.V. Mazurin, E.A. Porai-Koshits, *Phase separation in glass* (Elsevier, Amsterdam, North Holland, 1984).
[2] S. Morimoto, Key Eng. Mater., **115**, 147 (1996). DOI: 10.4028/www.scientific.net/KEM.115.147
[3] A.I. Beskrovny, S.G. Vasilovskii, S.B. Vakhrushev, D.A. Kurdyukov, O.I. Zvorykina, A.A. Naberezhnov, N.M. Okuneva, M. Tovar, E. Rysiakiewicz-Pasek, P. Jaguś, Phys. Solid State, **52** (5), 1092 (2010). DOI: 10.1134/S1063783410050410.
[4] L.N. Korotkov, V.S. Dvornikov, V.A. Dyad'kin, A.A. Naberezhnov, A.A. Sysoeva, Bull. Russ. Acad. Sci. Phys., **71** (10), 1404 (2007). DOI: 10.3103/S106287380710019X.
[5] A.A. Naberezhnov, S.B. Vakhrushev, Yu.A. Kumzerov, A.V. Fokin, Ferroelectrics, **575** (1), 75 (2021). DOI: 10.1080/00150193.2021.1888229
[6] S.V. Pan'kova, V.V. Poborchii, V.G. Solov'ev, J. Phys.: Condens. Matter, **8**, L203 (1996). DOI: 10.1088/0953-8984/8/12/001
[7] C. Tien, E.V. Charnaya, M.K. Lee, S.V. Baryshnikov, S.Y. Sun, D. Michel, W. Böhlmann, Phys. Rev. B, **72**, 104105 (2005). DOI: 10.1103/PhysRevB.72.104105
[8] E. Rysiakiewicz-Pasek, J. Komar, A. Cizman, R. Poprawski, J. Non-Cryst. Solids, **356**, 661 (2010). DOI: 10.1016/j.jnoncrysol.2009.07.035
[9] A.Y. Molokov, A.A. Sysoeva, A.A. Naberezhnye Chelny, E.Y. Koroleva, Nauchno-Tekh. Vedomosti S.-Peterb. Gos. Politekh. Univ. Fiz.-Mat. Nauki, **15** (3), 17 (2022) (in Russian). DOI: 10.18721/JPM.15302
[10] O.A. Alekseeva, A.A. Naberezhnov, A.A. Sysoeva, M.O. Enikeeva, Yu.E. Gorshkova, E.V. Lukin, Ferroelectrics, in press (2024). DOI: 10.1080/00150193.2024.2327953
[11] J. Teixeira, J. Appl. Cryst., **21**, 781 (1988). DOI: 10.1107/S0021889888000263
[12] H.D. Bale, P.W. Schmidt, Phys. Rev. Lett., **53**, 596 (1984). DOI: 10.1103/PhysRevLett.53.596
[13] M.V. Avdeev, V.L. Aksenov, Phys.-Usp., **53** (10), 971 (2010). DOI: 10.3367/UFNr.0180.201010a.1009 [M.V. Avdeev, V.L. Aksenov, Phys. Usp., **53** (10), 971 (2010). DOI: 10.3367/ufne.0180.201010a.1009].
[14] P. Wiltzius, F.S. Bates, S.B. Dierker, G.D. Wignall, Phys. Rev. A, **36** (6), 2991(R) (1987). DOI: 10.1103/PhysRevA.36.2991
[15] A. Höhr, H.-B. Neumann, P.W. Schmidt, P. Pfeifer, D. Avnir, Phys. Rev. B, **38** (2), 1462 (1988). DOI: 10.1103/PhysRevB.38.1462
[16] J.W. Cahn, Acta Met., **9** (9), 795 (1961). DOI: 10.1016/0001-6160(61)90182-1
[17] L.A. Feigin, D.I. Svergun, *Structure analysis by small-angle X-ray and neutron scattering* (Springer, N.Y., 1987).

Translated by D.Safin